Conductance through a Ti-atom impurity in Ag(100) and Au(111): An ionic model considering spin fluctuations

M. A. Romero,[1] C. S. Gómez Carrillo,[2] F. Flores,[3] and E. C. Goldberg[1,4]

[1]*Instituto de Desarrollo Tecnológico para la Industria Química (INTEC), Consejo Nacional de Investigaciones Científicas y Técnicas, Universidad Nacional del Litoral, Güemes 3450, CC 91, 3000 Santa Fe, Argentina*

[2]*Departamento de Física, Facultad de Ingeniería Química, Universidad Nacional del Litoral, Santiago del Estero 2829, 3000 Santa Fe Argentina*

[3]*Departamento Física Teórica de la Materia Condensada, Universidad Autónoma de Madrid, Madrid, Spain*

[4]*Departamento de Materiales, Facultad de Ingeniería Química, Universidad Nacional del Litoral, Santiago del Estero 2829, 3000 Santa Fe Argentina*

We describe the interaction between a transition-metal atom and a noble-metal surface by using an ionic model in which the first Hund's rule determines the filling of the atom's d levels, and spin fluctuations occur due to the electron exchange between the metal band and the atom states. We apply our model to the case of adsorbed Ti atoms on noble-metal surfaces (Ag and Au) in which conductance measurements in scanning tunneling microscope experiments suggest a mixed-valence regime according to the position and width of the atomic resonance. By introducing, in our calculation, these two parameters as extracted from the experiment, we satisfactorily reproduce the experimental results in both cases. We find, in the Ag(100) surface, that the conductance spectrum reflects electronic characteristics of the metal surface modified by the presence of the magnetic atom; whereas, in the Au(111) case, only the projected density of states on the Ti atom determines the conductance spectrum shape.

　　　PACS number(s): 72.10.−d, 75.20.Hr, 73.22.−f, 73.20.Hb

I. INTRODUCTION

The Kondo effect[1] and reminiscences of the Fano phenomena[2] have been detected in the conductance measurements of noble-metal surfaces with adsorbed 3d transition-metal atoms in scanning tunneling microscope (STM) experiments.[3–7] An experimental study of the temperature dependence of the Kondo resonance for an individual Ti atom resting on a Ag(100) surface was performed using a variable temperature STM over the temperature range of $T = 6$–49 K.[7] The spectrum obtained for $T = 6.8$ K was decomposed into a narrow Fano resonance at the Fermi level and a broader Fano resonance located slightly above the Fermi energy. The narrow resonance has a width of 10.5 mV, and it was identified as a Kondo resonance; whereas, the broader one has a width of 78 mV, and it was assumed to originate from a bare Ti d resonance.[7] The intrinsic local density of states (LDOS) for the Ti atom was obtained at different temperatures by thermally broadening the sum of the two Fano resonances before being fitted to each experimental spectrum. In this way, it was found that the Kondo component of the Ti LDOS broadens quadratically at low temperatures and follows a simple functional dependence that is well explained by the Fermi-liquid treatment of the Kondo effect.[7]

In an ensuing paper, Luo *et al.*[8] concluded that, in impurity systems, such as Ti atoms on Au (Ref. 6) or Ag (Ref. 7) surfaces, the line shape cannot be explained without invoking the interference between the Kondo resonance and the impurity level. However, in the mixed-valence regime where the impurity levels are located within the linewidth from the Fermi energy, the density of states at the Fermi level due to the broadening becomes significant, and a specific calculation for the impurity level in the mixed-valence regime should be performed.

The quantity calculated in Ref. 8 was the LDOS of the conduction electrons around the impurity site, which was obtained from the impurity Green's function using inaccurate expressions of the zero-order Green's function and of the scattering matrix as pointed out by Kolf *et al.*[9] Although Luo *et al.* corrected these problems, the fitting of the experimental curves shown in Ref. 10 did not change with respect to the one shown in the previous paper;[8] however, we have found that this fitting cannot be reproduced by means of the expressions and the parameters used in Ref. 10 (see the Appendix) as also discussed in Sec. III.

In the present paper, we calculate the LDOS for a Ti impurity atom on either Ag(100) or Au(111) surfaces by using an ionic model previously developed for analyzing the behavior of the Kondo resonances as a function of the d filling of transition-metal impurities.[11] The main assumptions are that the exchange energy is large enough to determine the atomic low-energy electronic configurations (first Hund's rule) and the *crystal-field terms* small compared with the energies related to the first Hund's rule. In this way, the local electronic structure of individual transition-metal impurities, having different d-level configurations on a Au surface, was appropriately reproduced.[6] In the Ti/Ag(100) system, we now find that the line shape of the measured conductance reflects electronic characteristics of the metal surface modified by the presence of the magnetic atom due to a non-negligible tip-substrate interaction,[12–16] whereas, in the case of Ti/Au(111), the interaction atom surface prevails, and the conductance line shape is only determined by the projected density of states on the Ti-atom impurity.

II. THEORY

In our approach, we introduce the following extended Anderson Hamiltonian:

$$H = H_{\text{leads}} + H_{\text{atom}} + H_{\text{int}} + H_{\text{tip substrate}}. \quad (1)$$

In Eq. (1), $H_{\text{leads}} = \sum_{k,\alpha,\sigma} \varepsilon_{k\alpha} \hat{c}^{\dagger}_{k\alpha\sigma} \hat{c}_{k\alpha\sigma}$ describes the free electrons of the leads where $\hat{c}^{\dagger}_{k\alpha\sigma}$ ($\hat{c}_{k\alpha\sigma}$) is the creation (annihilation) operator associated with the state $k\alpha\sigma$ ($\alpha = 1,2$ refers to the tip and the metal surface, respectively; σ is the spin projection), H_{atom} describes the d electrons of the atom, H_{int} designates the interaction between the $k\alpha\sigma$ and the d electrons, and $H_{\text{tip sustrate}}$ accounts for the tip-substrate interaction given by

$$H_{\text{tip sustrate}} = \sum_{k,k',\sigma} [w_{kk'} \hat{c}^{\dagger}_{k1\sigma} \hat{c}_{k'2\sigma} + \text{H.c.}]. \tag{2}$$

The critical point is the description of the d electrons; for a free atom, we consider the following Hamiltonian:

$$
\begin{aligned}
H_{\text{atom}} =& \sum_{m,\sigma} \varepsilon_m \hat{n}_{m\sigma} + \sum_m U_d \hat{n}_{m\uparrow} \hat{n}_{m\downarrow} + \frac{1}{2} \sum_{m \neq m',\sigma} J_d \hat{n}_{m\sigma} \hat{n}_{m'-\sigma} \\
&+ \frac{1}{2} \sum_{m \neq m',\sigma} (J_d - J^x_d) \hat{n}_{m\sigma} \hat{n}_{m'-\sigma} \\
&- \frac{1}{2} \sum_{m \neq m',\sigma} J^x_d \hat{c}^{\dagger}_{m\sigma} \hat{c}_{m-\sigma} \hat{c}^{\dagger}_{m'-\sigma} \hat{c}_{m'\sigma} \\
&+ \text{(crystalline-field terms)}. \tag{3}
\end{aligned}
$$

In Eq. (3), $\hat{n}_{m\sigma} = \hat{c}^{\dagger}_{m\sigma} \hat{c}_{m\sigma}$, and $\hat{c}^{\dagger}_{m\sigma}$ ($\hat{c}_{m\sigma}$) denotes the creation (annihilation) operator of the localized d electrons in the orbital m with spin σ. The intra-atomic Coulomb interactions U_d and J_d as well as the intra-atomic exchange interaction J^x_d are assumed to be constants independent of the m-orbital index. The fifth term, related to spin-flip processes, restores the invariance under rotation in spin space, and the last one has to be with the crystalline-field effects. In this representation, H_{int} is given by

$$H_{\text{int}} = \sum_{k,\alpha,m,\sigma} (V_{k\alpha m} \hat{c}^{\dagger}_{k\alpha\sigma} \hat{c}_{m\sigma} + \text{c.c.}), \tag{4}$$

where $V_{k\alpha m}$, spin independent, defines the coupling between the conduction $k\alpha\sigma$ and the localized $m\sigma$ electrons.

A crucial approximation to analyze Hamiltonian (3) is to assume the exchange interaction J^x_d to be large enough to make the first Hund's rule operative. Then, the atomic lower-energy configurations correspond to the states with a maximum electron spin, say S, compatible with the crystalline-field effects. Fluctuations associated with the Kondo resonance that take one electron from the leads and change the atomic wave function from $S - 1/2$ to S (for a less than half-filled atomic shell) are well contemplated by using the projector operator language.[17] In this approach, we can write Eqs. (3) and (4) in the following way:[11]

$$
\begin{aligned}
H_{\text{atom}} =& E_S \sum_M |S,M\rangle \langle S,M| \\
&+ E_{S-1/2} \sum_m |S - 1/2,m\rangle \langle S - 1/2,m| \\
H_{\text{int}} =& \sum_{k,\alpha,M,\sigma} [V_{k\alpha M\sigma} \hat{c}^{\dagger}_{k\alpha\sigma} |S - 1/2, M - \sigma\rangle \langle S,M| + \text{c.c.}]. \\
\tag{5}
\end{aligned}
$$

Here, $|S,M\rangle$ denotes the electronic configuration of the atom with total spin S and spin projection M, and

$$V_{k\alpha M\sigma} = \sqrt{\frac{[S + M^* \text{sgn}(\sigma)]}{10S}} V_{k\alpha}, \tag{6}$$

where $V_{k\alpha}$ is the sum over m of $V_{k\alpha m}$.[11] A similar approach has been used in the past for studying the valence fluctuations between two magnetic $4f$ configurations.[18]

By using *ab initio* calculations based on density functional theory, it was found[19–21] that $3d$ transition-metal atoms adsorbed in noble surfaces have $3d$ moments close to the atomic values given by Hund's first rule. Therefore, we consider the $S - 1/2 = 1$ to $S = 3/2$ spin fluctuation in the case of Ti adsorbed in Ag(100) and Au(111) surfaces.

All the physical magnitudes of interest related to the Ti/Ag and Ti/Au interacting systems can be obtained from the following Green's-Keldysh functions:[22]

$$
\begin{aligned}
G_{M\sigma}(t,t') =& i\Theta(t' - t)\langle \{ | \tfrac{3}{2}, M + \sigma \rangle \langle 1,M |_{(t')}; |1,M\rangle \\
&\times \langle \tfrac{3}{2}, M + \sigma |_{(t)} \} \rangle, \tag{7}
\end{aligned}
$$

$$F_{M\sigma}(t,t') = i\langle [| \tfrac{3}{2}, M + \sigma \rangle \langle 1,M |_{(t')}; |1,M\rangle \langle \tfrac{3}{2}, M + \sigma |_{(t)}] \rangle, \tag{8}$$

by taking into account the norm condition within the selected configuration subspace,

$$\sum_M | \tfrac{3}{2}, M \rangle \langle \tfrac{3}{2}, M | + \sum_m |1,m\rangle \langle 1,m| = \hat{1}. \tag{9}$$

In Eqs. (7) and (8), the $\{;\}$ and $[;]$ symbols denote anticonmutator and conmutator, respectively. The F functions provide the atom-state occupation in the nonequilibrium situations.[17]

A. Current and conductance calculation

We assume two leads, 1 (the tip) and 2 (the metal surface). The current in the tip, for instance, is determined by the time variation in the total electron charge (e being the elemental charge unit),

$$I^{\sigma}_{\text{tip}} = -e \frac{d}{dt} \sum_k \langle \hat{n}_{k1\sigma} \rangle = \frac{ie}{\hbar} \sum_k \langle [\hat{c}^{\dagger}_{k1\sigma} \hat{c}_{k1\sigma}, \hat{H}] \rangle.$$

By solving the conmutator, we obtain the following expression:

$$
\begin{aligned}
I^{\sigma}_{\text{tip}} =& \frac{2e}{\hbar} \text{Im} \sum_k \left[\sum_M V^*_{k1M\sigma} \langle | \tfrac{3}{2}, M + \sigma \rangle \langle 1,M | \hat{c}_{k1\sigma} \rangle \right. \\
&\left. + \sum_{k'} w^*_{kk'} \langle c^{\dagger}_{k'2\sigma} c_{k1\sigma} \rangle \right]_t, \tag{10}
\end{aligned}
$$

where $V_{k\alpha M\sigma}$ is given by Eq. (6). The crossed terms involving the atom states are calculated by using the following Green's functions:

$$F_{M\sigma}[\hat{c}_{k1\sigma}(t)] = i\left\langle\left[\left|\tfrac{3}{2}, M+\sigma\right\rangle\langle 1, M_{(t')}|; \hat{c}_{k1\sigma}(t)\right]\right\rangle,$$

$$F_{\hat{c}^\dagger_{k'2\sigma}}[\hat{c}_{k1\sigma}(t)] = i\langle[\hat{c}^\dagger_{k'2\sigma}(t'); \hat{c}_{k1\sigma}(t)]\rangle \quad (11)$$

evaluated at equal time values $t = t'$, accordingly with the expressions,

$$\left\langle\left|\tfrac{3}{2}, M+\sigma\right\rangle\langle 1, M|_t\, \hat{c}_{k1\sigma}(t)\right\rangle = \frac{F_{M\sigma}(c_{k1\sigma})}{2i},$$

$$\langle\hat{c}^\dagger_{k'2\sigma}(t)\,\hat{c}_{k1\sigma}(t)\rangle = \frac{F_{\hat{c}^\dagger_{k'2\sigma}}(c_{k1\sigma})}{2i}. \quad (12)$$

We are interested in calculating the current in the tunneling regime with respect to the tip-atom and tip-substrate interactions. Therefore, the equations of motion of these Green's functions are solved by conserving only terms that lead to a second-order approximation in V_{k1} and $w_{kk'}$ of Eq. (10),

$$i\frac{d}{dt}F_{M\sigma}[\hat{c}_{k1\sigma}(t)] = \varepsilon_{k1}F_{M\sigma}[\hat{c}_{k1\sigma}(t)] + V_{k1M\sigma}F_{M\sigma}(t,t')$$
$$+ \sum_{k'} w_{kk'}F_{M\sigma}[\hat{c}_{k'2\sigma}(t)]. \quad (13)$$

We integrate Eqs. (13) by using the boundary condition at the initial time $t = t_0$ (noninteracting systems) which relates the F function to the advanced Green's function G,

$$F_{M\sigma}[\hat{c}_{k\alpha\sigma}(t_0)] = [2\langle\hat{n}_{k\alpha\sigma}(t_0)\rangle - 1]G_{M\sigma}[\hat{c}_{k\alpha\sigma}(t_0)],$$

where $\langle\hat{n}_{k\alpha\sigma}(t_0)\rangle = (e^{(\varepsilon_{k\alpha}-\varepsilon_{F\alpha})/k_BT}+1)^{-1} = f_<(\varepsilon_{k\alpha}-\varepsilon_{F\alpha})$ is the Fermi function at temperature T ($\varepsilon_{F\alpha}$ is the Fermi energy

of the lead α). This yields

$$F_{M\sigma}(c_{k1\sigma}) = -i\int_{t_0}^t d\tau\, V_{k1M\sigma}(\tau)\{F_{M\sigma}(\tau,t)$$
$$- \xi_{k1\sigma}G_{M\sigma}(\tau,t)\}e^{-i\int_\tau^t \varepsilon_{k1}(\tau')d\tau'}$$
$$- i\sum_{k'}\int_{t_0}^t d\tau\, w_{kk'}(\tau)\{F_{M\sigma}[c_{k'2\sigma}(\tau)]$$
$$- \xi_{k1\sigma}G_{M\sigma}[c_{k'2\sigma}(\tau)]\}e^{-i\int_\tau^t \varepsilon_{k1}(\tau')d\tau'}, \quad (14)$$

where we have defined $\xi_{k1\sigma} = [2\langle n_{k1\sigma}(t_0)\rangle - 1]$.

By following a similar procedure, we arrive at the following expression for $F_{\hat{c}^\dagger_{k'2\sigma}}[\hat{c}_{k1\sigma}(t)]$ at equal time values $t = t'$:

$$F_{\hat{c}^\dagger_{k'2\sigma}}(\hat{c}_{k1\sigma})$$
$$= -i\sum_{k''}\int_{t_0}^t d\tau\, w_{kk''}\{F_{\hat{c}^\dagger_{k'2\sigma}}[c_{k''2\sigma}(\tau)]$$
$$- \xi_{k1\sigma}G_{\hat{c}^\dagger_{k'2\sigma}}[c_{k''2\sigma}(\tau)]\}e^{-i\int_\tau^t \varepsilon_{k1}(\tau')d\tau'}$$
$$- i\sum_M\int_{t_0}^t d\tau\, V_{k1M\sigma}\left\{F_{\hat{c}^\dagger_{k'2\sigma}}\left(|1,M\rangle\langle\tfrac{3}{2},M+\sigma|_\tau\right)\right.$$
$$\left. - \xi_{k1\sigma}G_{\hat{c}^\dagger_{k'2\sigma}}\left(|1,M\rangle\langle\tfrac{3}{2},M+\sigma|_\tau\right)\right\}e^{-i\int_\tau^t \varepsilon_{k1}(\tau')d\tau'}. \quad (15)$$

Equations (10), (12), (14), and (15) yield I^σ_{tip}. In the stationary case, by considering the Fourier transform of the Green's functions and using the identity,

$$\text{Im}\int_{-\infty}^\infty d\omega\frac{[F - \xi_{k1\sigma}G]}{\omega - \varepsilon_k + i\eta}$$
$$= \int_{-\infty}^\infty d\omega\,\text{Im}\{F - 2\xi_{k1\sigma}G\}\pi\delta(\omega - \varepsilon_k), \quad (16)$$

we obtain the following equation:[23]

$$\frac{I^\sigma_{\text{tip}}}{e/h} = \text{Im}\left\{\frac{6}{15}\Gamma_{\text{at}}\int_{-\infty}^\infty d\omega\,[F_{1\sigma} - 2\xi_{1\sigma}G_{1\sigma}] + \sum_{M,k''}\Gamma^{M\sigma}_{\text{ats}}\int_{-\infty}^\infty d\omega\,[F_{M\sigma}(\hat{c}_{k''2\sigma}) - 2\xi_{1\sigma}G_{M\sigma}(\hat{c}_{k''2\sigma})]\right.$$
$$+ \sum_{M,k''}\Gamma^{M\sigma*}_{\text{ats}}\int_{-\infty}^\infty d\omega\left[F_{\hat{c}^\dagger_{k''2\sigma}}\left(|1,M\rangle\langle\tfrac{3}{2},M+\sigma|\right) - 2\xi_{1\sigma}G_{\hat{c}^\dagger_{k''2\sigma}}\left(|1,M\rangle\langle\tfrac{3}{2},M+\sigma|\right)\right]$$
$$\left. + \sum_{k',k''}\Gamma_{\text{ts}}\int_{-\infty}^\infty d\omega\left[F_{\hat{c}^\dagger_{k'2\sigma}}(\hat{c}_{k''2\sigma}) - 2\xi_{1\sigma}G_{\hat{c}^\dagger_{k'2\sigma}}(\hat{c}_{k''2\sigma})\right]\right\}, \quad (17)$$

where now $\xi_{1\sigma} = [2f_<(\omega - \varepsilon_{F_1}) - 1]$ with $\varepsilon_{F_1} = \varepsilon_F + V$, ε_F is the Fermi energy of the system at equilibrium, and V is the applied bias voltage. The following quantities have been introduced in Eq. (17) by neglecting the k dependence of the atom-surface coupling terms and assuming a flat density of states of the tip (ρ_{tip}) around the Fermi level:

$$\Gamma_{\text{at}} = \pi\sum_k |V_{k1}|^2\delta(\varepsilon - \varepsilon_{k1}) \approx \pi|V_1|^2\rho_{\text{tip}},$$

$$\Gamma^{M\sigma}_{\text{ats}} = \pi\sum_k V^*_{k1M\sigma}w_{k'k}\delta(\varepsilon - \varepsilon_{k1}) \approx \pi V^*_{1M\sigma}w\rho_{\text{tip}},$$

$$\Gamma_{\text{ts}} = \pi\sum_k w^*_{k'k}w_{k''k}\delta(\varepsilon - \varepsilon_{k1}) \approx \pi|w|^2\rho_{\text{tip}}.$$

By also assuming that the atom-tip interaction is negligible with respect to the atom-surface interaction, we can write $\text{Im}\,F(\omega) = 2[2f(\omega - \varepsilon_F) - 1]\text{Im}\,G(\omega)$, finally arriving at the expression,

$$\frac{I^\sigma_{\text{tip}}}{2e^2/h} = 2\,\text{Im}\left\{\frac{6}{15}\int_{-\infty}^\infty d\omega\,[f_<(\omega - \varepsilon_F) - f_<(\omega - \varepsilon_F - V)]\,\Gamma_{\text{at}}G_{1\sigma}(\omega)\right.$$
$$+ \sum_{M,k''}\int_{-\infty}^\infty d\omega\,[f_<(\omega - \varepsilon_F) - f_<(\omega - \varepsilon_F - V)]\,\Gamma^{M\sigma}_{\text{ats}}G_{M\sigma}(\hat{c}_{k''2\sigma})$$

$$+ \sum_{m,k''} \int_{-\infty}^{\infty} d\omega \left[f_<(\omega - \varepsilon_F) - f_<(\omega - \varepsilon_F - V) \right] \Gamma_{\text{ats}}^{M\sigma} G_{\hat{c}_{k''2\sigma}^\dagger} \left(|1,M\rangle \langle \tfrac{3}{2}, M+\sigma| \right)$$

$$+ \sum_{k',k''} \int_{-\infty}^{\infty} d\omega \left[f_<(\omega - \varepsilon_F) - f_<(\omega - \varepsilon_F - V) \right] \Gamma_{\text{ts}} G_{\hat{c}_{k'2\sigma}^\dagger} (\hat{c}_{k''2\sigma}) \Bigg\} . \tag{18}$$

Equation (18) provides us the tunneling current without any approximation related to the atom-substrate interaction.

B. Green's functions calculation: Equation of motion method

The equations of motion of the crossed Green's functions appearing in Eq. (18) are solved up to a second order in the coupling with the substrate (V_{k2}) and by conserving only diagonal terms,

$$\sum_{k''} G_{M\sigma} (\hat{c}_{k''2\sigma}) = \sum_{k''} \frac{V_{k''2M\sigma}}{\varpi - \varepsilon_{k''2}} G_{M\sigma},$$

$$\sum_{k'} G_{\hat{c}_{k'2\sigma}^\dagger} \left(|1,M\rangle \langle \tfrac{3}{2}, M+\sigma| \right) = \sum_{k'} \frac{V_{k'2M\sigma}^*}{\varpi - \varepsilon_{k'2}} G_{M\sigma}, \tag{19}$$

$$\sum_{k',k''} G_{\hat{c}_{k'2\sigma}^\dagger} (\hat{c}_{k''2\sigma}) = \sum_{k'} \frac{1}{\varpi - \varepsilon_{k'2}} + \frac{6}{15} \sum_{k''} \frac{V_{k''2}}{\varpi - \varepsilon_{k''2}} G_{1\sigma} \sum_{k'} \frac{V_{k'2}^*}{\varpi - \varepsilon_{k'2}}.$$

We now introduce Eqs. (19) into Eq. (18) and neglect the k dependence of the atom-surface coupling term; by taking into account that the unperturbed substrate Green's function is given by $G_0^S = \sum_{k''} \frac{1}{\omega - \varepsilon_{k''2} - i\eta}$, we arrive at the following expression for the conductance at low bias voltage values:

$$\frac{G}{G_0} = 4 \left\{ \frac{6}{15} \int_{-\infty}^{\infty} d\omega\, \Gamma_{\text{at}} \text{Im}\, G_{1\sigma} \frac{d}{d\omega} f_<(\omega - \varepsilon_F) + \frac{6}{15} V_2 \int_{-\infty}^{\infty} d\omega\, \Gamma_{\text{ats}}^\sigma \text{Im} \left[G_0^S G_{1\sigma} \right] \frac{d}{d\omega} f_<(\omega - \varepsilon_F) \right.$$

$$\left. + \frac{6}{15} V_2^* \int_{-\infty}^{\infty} d\omega\, \Gamma_{\text{ats}}^{\sigma*} \text{Im} \left[G_0^S G_{1\sigma} \right] \frac{d}{d\omega} f_<(\omega - \varepsilon_F) + \int_{-\infty}^{\infty} d\omega\, \Gamma_{\text{ts}} \text{Im} \left[G_0^S + \frac{6}{15} |V_2|^2 G_0^S G_{1\sigma} G_0^S \right] \frac{d}{d\omega} f_<(\omega - \varepsilon_F) \right\}, \tag{20}$$

with $\Gamma_{\text{ats}}^\sigma = \pi V_1^* w \rho_{\text{tip}}$ and $G_0 = 2e^2/h$, the quantum of conductance.

Finally, by assuming a flat substrate density of states around the Fermi energy, we can write (20) as[17]

$$\frac{G}{G_0} = 4\pi \Gamma_{\text{ts}} \rho_{\text{sus}} \int_{-\infty}^{\infty} d\omega \left[1 + \frac{6}{15} \Gamma_{as} \left\{ (q^2 - 1) \text{Im}\, G_{1\sigma} + 2q\, \text{Re}\, G_{1\sigma} \right\} \right] \frac{d}{d\omega} f_<(\omega - \varepsilon_F), \tag{21}$$

where $\Gamma_{as} = \pi |V_2|^2 \rho_{\text{sus}}$ with $\rho_{\text{sus}} = \text{Im}\, G_0^S / \pi$ and $q = V_1 / w V_2 \pi \rho_{\text{sus}} + \text{Re}\, G_0^S / \text{Im}\, G_0^S$.

In the case of a negligible coupling between the tip and the substrate ($w \to 0$), we have that $q \approx V_1 / w V_2 \pi \rho_{\text{sus}} \gg 1$, and the conductance at low voltages and low temperatures is determined by the impurity spectral density around the Fermi energy:

$$\frac{G}{G_0} = 4\Gamma_{\text{at}} \int_{-\infty}^{\infty} d\omega \frac{6}{15} \text{Im}\, G_{1\sigma} \frac{d}{d\omega} f_<.$$

In the opposite limit, the coupling tip substrate w is the dominant one, $q \approx q_c = \text{Re}\, G_0^S / \text{Im}\, G_0^S$, and the microscope probe only "sees" the local change in the substrate density of states produced by the interaction with the impurity atom.[6] In this case,

$$\frac{G}{G_0} = 4\Gamma_{\text{ts}} \int_{-\infty}^{\infty} d\omega\, \text{Im} \left[G_0^S + \frac{6}{15} |V_2|^2 G_0^S G_{1\sigma} G_0^S \right] \frac{d}{d\omega} f_<(\omega).$$

Finally, the required Green's function in Eq. (21) is calculated by solving its equation of motion up to second order in the coupling with the substrate (V_{k2}) as explained in Ref. 11, neglecting the tip-atom interaction V_{k1}. For the nonmagnetic substrate case, the expression is as follows:

$$\left[\omega - \varepsilon_I - \frac{1}{5} \sum_k \frac{V_{k2}^2}{\varpi - \varepsilon_{k2}} - \frac{1}{15} \sum_k \frac{V_{k2}^2 f_<(\varepsilon_{k2} - \varepsilon_{F2})}{\varpi - \varepsilon_{k2}} \right] G_{1\sigma}(\varpi)$$

$$= \langle |3/2, 3/2\rangle \langle 3/2, 3/2| + |1,1\rangle \langle 1,1| \rangle - \frac{1}{15\pi} \sum_k \frac{V_{k2}^2}{\varpi - \varepsilon_{k2}} \int_{-\infty}^{\infty} d\omega'\, f_<(\omega' - \varepsilon_{F2}) \text{Im} \frac{G_{1\sigma}(\omega')}{\varpi' - \varepsilon_{k2}}, \tag{22}$$

where $\varepsilon_I = E_{3/2} - E_1$ and $\varpi \equiv \omega - i\eta$ with $\eta \to 0$. In all the integrals in Eq. (22), we have considered $\text{Im} \sum_k \frac{V_{k2}^2}{\varpi - \varepsilon_{k2}} = \Gamma_{as} = \pi |V_2|^2 \rho_{\text{sus}}$.

III. RESULTS AND DISCUSSION

A. Ti in Ag (100)

In this case, $\varepsilon_I = -20$ and $\Gamma_{as} = 120$ meV were chosen for reproducing the characteristics of the observed conductance spectrum[7] (the position of the d resonance and the widths of both broad and narrow resonances); the half-width of the d resonance in our model is given by $\Gamma = (\frac{1}{5} + \frac{1}{15})\Gamma_{as}$ for Eqs. (22) accordingly. The local density of states at the Ti impurity atom, $\rho_d(\omega) = \frac{1}{\pi}\text{Im}\,G_{1\sigma}(\omega)$, is shown in Fig. 1 for a temperature of $T = 6.8$ K.

This is a mixed-valence regime evolving from a Kondo regime, corresponding to a relation $\varepsilon_I/2\Gamma = -0.3$; the probabilities of occurrence of the electronic configurations with $S = 3/2$ and $S = 1$ given by $\sum_M \langle |S,M\rangle \langle S,M| \rangle$ are 0.55 and 0.45, respectively.

The measured conductance[7] is well fitted by using the expression (21) together with values of q between 1.8 and 2.4 ($q_c = 1.2$) and Γ_{ts} between 0.1 and 0.07 meV as shown in Fig. 2.

In Fig. 3, we compare our best result obtained for $q = 1.8$ (slightly displaced on the x axis in order to get a better adjustment to the experimental curve) with the theoretical proposal of Luo *et al.*[8,10] based on their Eqs. (A1)–(A4) and the corresponding set of parameters for Ti/Ag presented in the Appendix. As we can see from Fig. 3, the excellent fit of the experimental data shown in Ref. 10 is far from being reproduced by using the corresponding expressions and parameters of Refs. 8 and 10. On the other hand, our proposal, based on an ionic model in which the first Hund's rule is imperative, provides a very good description of the measured conductance when including the tip-metal surface interaction. In the case of Ti interacting with Ag(100), this interaction is important but is not dominant ($q \approx 2$); therefore, the microscope probe is sensing both the tip-atom and the tip-metal currents.

The dependence of the conductance with the temperature is shown in Fig. 4 where we can observe that the general trends of the experimental results[7] are well reproduced.

FIG. 2. (Color online) The conductance as a function of the applied voltage for Ti/Ag(100). Our calculations, Eqs. (21) and (22), for different q values: 1.8 (solid black line), 2.0 (solid gray line), 2.2 (dashed line), and 2.4 (dotted line). Empty circles correspond to the experimental curve from Ref. 7.

In the case of Ti atoms adsorbed in Ag(100), the impurity level is located within the linewidth from the Fermi energy, and the density of states at the Fermi level due to the d resonance becomes significant. Therefore, within this mixed-valence regime, it is not possible to separate the contribution provided by the d-resonance broadening from that provided by the strong correlation effects around the Fermi energy. We adopted the following criterion for defining a temperature dependence of the width of the low-energy resonance peak from the change in the local density of states in the Ti atom with temperature: the full width at half maximum of the resonance peak is measured with respect to the horizontal line indicated in Fig. 5.

FIG. 3. (Color online) The conductance as a function of the applied voltage for Ti/Ag(100). Comparison of our result for $q = 1.8$ (solid line) with the one obtained with expressions (A1)–(A4) and parameter values given in the Appendix[8,10] (dotted line). Open circles correspond to the experimental result from Ref. 7.
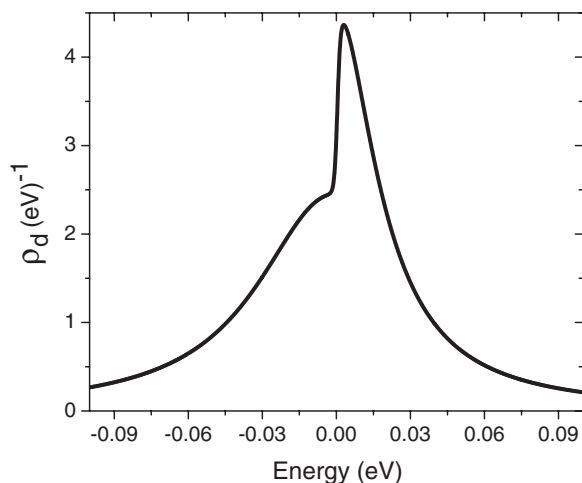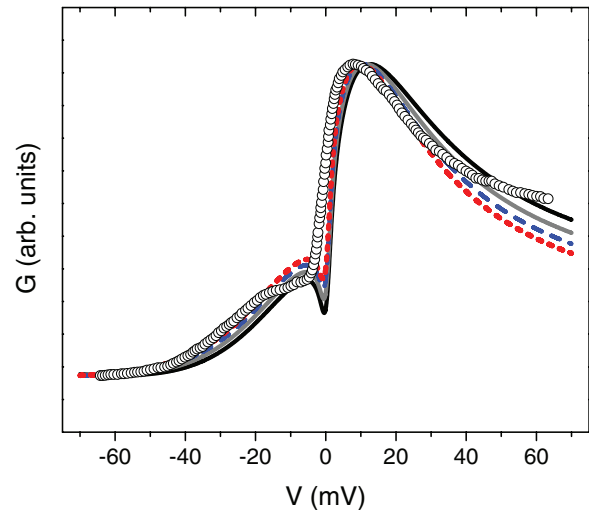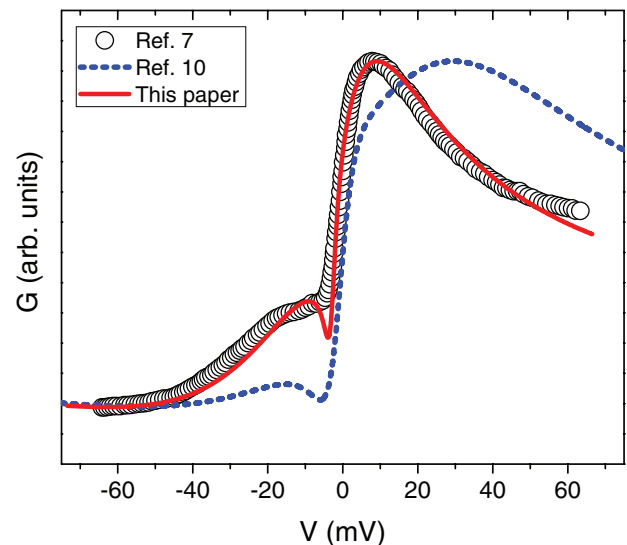

FIG. 1. Local density of states for the Ti impurity atom in Ag(100) calculated by using the ionic model Hamiltonian (1).
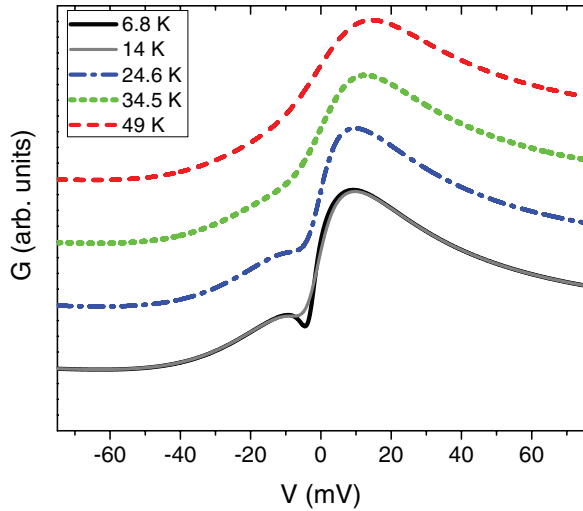
FIG. 4. (Color online) The calculated conductance spectrum for Ti/Ag(100) as a function of the applied voltage for several temperature values.

We found that the width calculated in this form increases quadratically at low temperatures but becomes a linear function as the temperature is raised above 30 K, a similar result to the one discussed in Ref. 7. We also found that the temperature dependence of the resonance width for $T < 50$ K is well fitted by the expression $2\Gamma_K = \sqrt{(\alpha k_B T)^2 + (2k_B T_K)^2}$ with $\alpha = 2.56$ and $T_K = 63$ K as shown in the inset of Fig. 5. In the same figure, we can see that raising the temperature suppresses the Kondo effect, causing the peak to approach the position of the bare resonance. The renormalized d level of half-width $\Gamma \approx 32$ meV acquires a strong temperature dependence on a scale of $T \approx \Gamma$, a typical behavior of the mixed-valence regime.[24]

B. Ti in Au(111)

The shape and width of the measured conductance spectrum in this case[6] is well reproduced by choosing $\varepsilon_I = 10$,
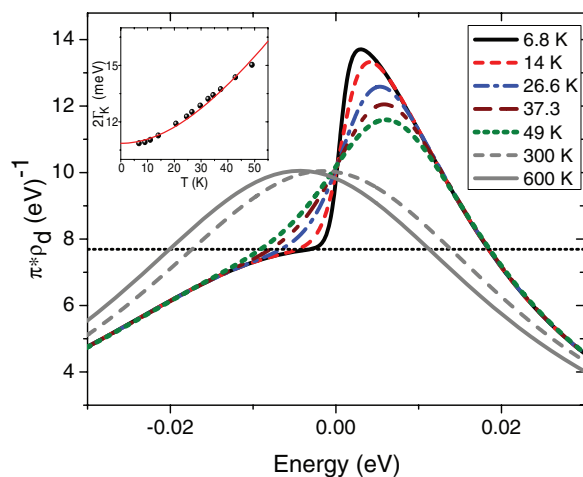

FIG. 5. (Color online) Temperature dependence of the local density of states for the impurity Ti atom in Ag(100). The low-energy resonance width as a function of temperature is shown in the inset.
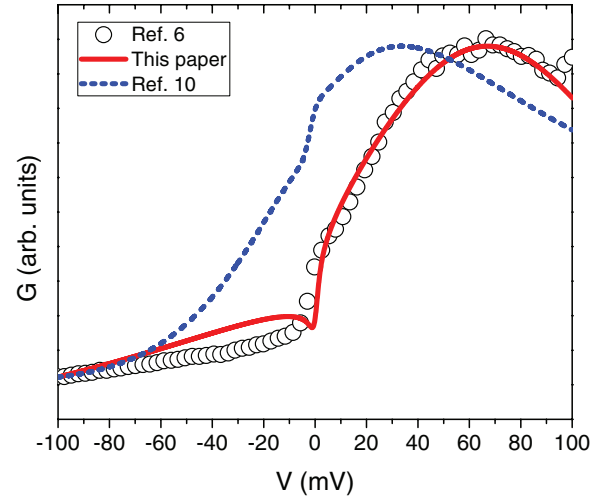

FIG. 6. (Color online) The conductance as a function of the applied voltage for Ti/Au(111). Comparison of our result [Eqs. (21) and (22)] for $q \gg 1$ (solid line) with the one obtained with expressions (A1)–(A4) and parameter values given in the Appendix[8,10] (dotted line). Open circles correspond to the experimental result from Ref. 6.

$\Gamma_{as} = 500$ meV, and considering the limit $q \gg 1$. Therefore, in the Au substrate case ($q_c = 2.2$), the observed conductance spectrum around the Fermi level is practically determined by the local density of states in the Ti atom as we can see in Fig. 6. The theoretical curve resulting from Eqs. (A1)–(A4) and the corresponding set of parameters for Ti/Au in the Appendix is also shown in Fig. 6. It can be observed, as in the Ti/Ag case, that the excellent fit of the experimental data shown in Ref. 10 is far from being reproduced.

In the Ti/Au (111) system, a mixed-valence regime evolving to an empty orbital regime is found; in this case, $\Gamma = \Gamma_{as}/5$ and $\varepsilon_I/2\Gamma = 0.05$. The $S = 1$ configuration has a larger probability of occurrence (0.64) than the electronic configuration with $S = 3/2$ (0.36). In Fig. 7,
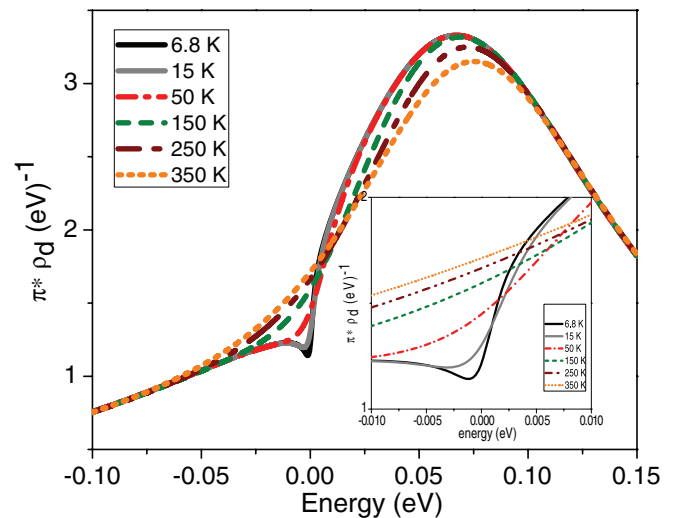

FIG. 7. (Color online) Temperature dependence of the local density of states for the impurity Ti atom in Au (111). The inset is a blowup of the near-to-zero energy values.

the temperature dependence of the local density of states in the Ti atom is shown. We can observe that the slightly insinuated Kondo structure, which appears merged into the atomic resonance at very low energy, disappears for $T > 50$ K (see the inset in Fig. 7) and that the resonance peak tends to the renormalized d level of half-width $\Gamma \approx 100$ meV.

IV. CONCLUSIONS

The Ti impurity atom in both Ag(100) and Au(111) surfaces is described by using an ionic Hamiltonian and assuming the d-orbital occupancy determined by the first Hund's rule. The electron exchange between the atom-level and the surface-band states makes the total atom spin S fluctuate between $S = 1$ and $S = 3/2$. The position and width of the atomic resonance used in our model are extracted from the measured conductance spectra.[6,7] In this form, the mixed valence expected in both cases, Ti/Ag and Ti/Au, satisfactorily reproduces the characteristics of the observed conductance spectra shape and the temperature dependence.

We should also comment that the solution presented for the equation of motion method up to second order in V_k, as discussed in Sec. II B, provides a good description of the mixed-valence regime, namely, when the resonance is close to the Fermi energy ($|\varepsilon_I - \varepsilon_F| < \Gamma$).[25] In the Ti/Ag case for which the mixed-valence regime is near the crossover with the Kondo regime, the line shape of the measured conductance reflects electronic characteristics of the metal surface modified by the presence of the magnetic atom. In the Ti/Au case, the mixed-valence regime is near the crossover with the empty orbital regime, and the conductance spectrum shape is determined mainly by the local density of states in the Ti atom.

APPENDIX

Luo *et al.*[8] proposed that the physical quantity measured by the STM is essentially the local density of states of conduction electrons around the impurity site [Eq. (3) of Ref. 8],

$$\delta\rho_c(r,\omega) = -\Delta\rho_0 \left[(q_c^2 - 1) \, \mathrm{Im} \, G_d(\omega) - 2q_c \, \mathrm{Re} \, G_d(\omega) \right],$$
(A1)

with the impurity Green's function $G_d(\omega)$ given by [Eq. (4) of Ref. 8],

$$G_d(\omega) = G_d^0(\omega) + G_d^0(\omega) T_d(\omega) G_d^0(\omega),$$
(A2)

where $q_c = -\mathrm{Re} \, G_c^0(\omega) / \mathrm{Im} G_c^0(\omega)$ and $G_c^0(\omega)$ is the retarded Green's function for the nonperturbed conduction electrons. In the infinite correlation limit ($U \to \infty$) [Eq. (5) of Ref. 8],

$$G_d^0(\omega) = \frac{1 - n/2}{\omega - \varepsilon_d + i\Delta},$$
(A3)

and the expression used for the scattering matrix [Eq. (1) of Ref. 10] is as follows:

$$T_d(\omega) = \frac{a e^{i\delta}}{\omega - \varepsilon_K + i\Gamma_K}.$$
(A4)

The fitting parameters are $(n, \varepsilon_d, \Delta, \varepsilon_K, \Gamma_K, a, \delta, q_c) = (0.38; 2.3; 65.0; -1.9; 4.0; 28.2; 2.7; 2.0)$ for Ti/Au and $(0.53; 13.4; 38.8; -1.4; 5.2; 144.9; 3.0; 1.8)$ for Ti/Ag (the Fermi energy $\varepsilon_F = 0$ and the unit of energy is meV).[10]

[1] U. Fano, Phys. Rev. **124**, 1866 (1961).

[2] J. Kondo, Prog. Theor. Phys. **32**, 37 (1964).

[3] V. Madhavan, W. Chen, T. Jamneala, M. F. Crommie, and N. S. Wingreen, Science **280**, 567 (1998).

[4] J. Li, W.-D. Schneider, R. Berndt, and B. Delley, Phys. Rev. Lett. **80**, 2893 (1998).

[5] H. C. Manoharan, C. P. Lutz, and D. M. Eigler, Nature (London) **403**, 512 (2000).

[6] T. Jamneala, V. Madhavan, W. Chen, and M. F. Crommie, Phys. Rev. B **61**, 9990 (2000).

[7] K. Nagaoka, T. Jamneala, M. Grobis, and M. F. Crommie, Phys. Rev. Lett. **88**, 077205 (2002).

[8] H. G. Luo, T. Xiang, X. Q. Wang, Z. B. Su, and L. Yu, Phys. Rev. Lett. **92**, 256602 (2004).

[9] C. Kolf, J. Kroha, M. Ternes, and W.-D. Schneider, Phys. Rev. Lett. **96**, 019701 (2006).

[10] H. G. Luo, T. Xiang, X. Q. Wang, Z. B. Su, and L. Yu, Phys. Rev. Lett. **96**, 019702 (2006).

[11] E. C. Goldberg and F. Flores, Phys. Rev. B **77**, 125121 (2008).

[12] V. Madhavan, W. Chen, T. Jamneala, M. F. Crommie, and N. S. Wingreen, Phys. Rev. B **64**, 165412 (2001).

[13] M. Plihal and J. Gadzuk, Phys. Rev. B **63**, 085404 (2001).

[14] J. Merino and O. Gunnarsson, Phys. Rev. Lett. **93**, 156601 (2004).

[15] J. Merino and O. Gunnarsson, Phys. Rev. B **69**, 115404 (2004).

[16] K. R. Patton, S. Kettemann, A. Zhuravlev, and A. Lichtenstein, Phys. Rev. B **76**, 100408 (2007).

[17] A. C. Hewson, *The Kondo Problem to Heavy Fermions* (Cambridge University Press, Cambridge, UK, 1993).

[18] A. A. Aligia, C. A. Balseiro, and C. R. Proetto, Phys. Rev. B **33**, 6476 (1986).

[19] B. Nonas, I. Cabria, R. Zeller, P. H. Dederichs, T. Huhne, and H. Ebert, Phys. Rev. Lett. **86**, 2146 (2001).

[20] I. Cabria, B. Nonas, R. Zeller, and P. H. Dederichs, Phys. Rev. B **65**, 054414 (2002).

[21] S. Blügel and P. H. Dederichs, Europhys. Lett. **9**, 597 (1989).

[22] V. Keldysh, Zh. Eksp. Teor. Fiz. **47**, 1515 (1964) [Sov. Phys. JETP **20**, 1018 (1965)].

[23] A.-P. Jauho, N. S. Wingreen, and Y. Meir, Phys. Rev. B **50**, 5528 (1994).

[24] T. A. Costi, A. C. Hewson, and V. Zlatic, J. Phys.: Condens. Matter **6**, 2519 (1994).

[25] E. C. Goldberg, F. Flores, and R. Monreal, Phys. Rev. B **71**, 035112 (2005); R. Monreal and F. Flores, *ibid.* **72**, 195105 (2005).